Contents lists available at Science-Gate

International Journal of Advanced and Applied Sciences

Journal homepage: http://www.science-gate.com/IJAAS.html

Influence of graphene nano-strips on the vibration of thermoelastic nanobeams

Mohammad Salem J. Alzahrani [1], Najat A. Alghamdi [2,*], Jamiel A. Alotaibi [2,3]

[1]*Electronic and Communications Department, College of Engineering– Al-Leith, Umm Al-Qura University, Makkah, Saudi Arabia*
[2]*Mathematics Department, College of Applied Science, Umm Al-Qura University, Makkah, Saudi Arabia*
[3]*Mathematics Department, College of Applied Science, Taif University, Taif, Saudi Arabia*

ARTICLE INFO

Article history:
Received 1 June 2023
Received in revised form
24 September 2023
Accepted 28 November 2023

Keywords:
Thermo-electrical effect
Graphene nano-strip
Thermoelasticity
Vibration
Green-Naghdi model

ABSTRACT

This research deals with the investigation of the vibrational behavior of thermoelastic homogeneous isotropic nanobeams, with particular emphasis on the application of non-Fourier heat conduction theory. The nanobeam is configured with one end having a graphene nano-strip connected to an electrical source supplying a low voltage current. To analyze this system, the Green-Naghdi type I and type III theorems are applied within the framework of simply supported boundary conditions while maintaining a fixed aspect ratio. The nanobeam is subjected to thermal loading due to the heat generated by the current flow through the graphene nano-strip. The governing equations are solved in the Laplace transform domain, and the inverse Laplace transform is computed numerically using Tzou's approximation method. Our results, as shown in the figures, reveal different scenarios characterized by varying electric voltage and electric resistance values for the nanographene strips. It is evident that these parameters exert a profound influence on the functional behavior of the nanobeam, thus providing a mechanism to regulate both its vibrational characteristics and temperature rise through judicious manipulation of the electrical voltage and resistance levels.

1. Introduction

The theory of coupled thermoelasticity is a type of heat conduction and has been proven to serve several problems (Tzou, 1989). This theory consists of two partial differential equations, the equation of motion and the law of conservation of energy, based on Fourier's law of heat conduction (Alghamdi, 2016; Alghamdi, 2020a; 2020b; Alghamdi and Youssef, 2017; Biot, 1956; Youssef and Alghamdi, 2015). This type of heat conduction increases the propagation velocity of heat waves infinitely. Lord and Shulman (Lord and Shulman, 1967) proposed a generalized theory of thermoelasticity with relaxation time for isotropic objects. In this theory, the heat conduction law is modified so that the inclusion of both heat flow and its time derivative (Cattaneo's law or non-Fourier's law of heat conduction) replaces Fourier's law. Since the heat equation of this theory is a hyperbola, it removes the paradox of infinite propagation velocity (Dhaliwal and Sherief, 1980).

In recent years, many scientists have dealt with micro/nano electric machines. There are many applications based on micro/nanoelectromechanical beam resonators, such as actuators, beams, sensors, pumps, resonators, and motors, and even very important for physical applications (Hoang, 2015; Naik et al., 2009; O'Connell et al., 2010; Van Beek and Puers, 2011).

It is important to study thermoelastic vibration micro/nanobeam resonators. Alghamdi (2016) studied thermoelastic damping in rectangular microplate resonators using the generalization theory of thermoelasticity with the two-temperature theory. Sharma and Grover (2011) studied the lateral oscillations of thin, homogeneous, isotropic, thermoelastic micro/nanoscale thin beam cavity resonators. Sun and Saka (2010) studied the vibration damping of thermoelastic disk resonators off the plane of the microplate. They introduced a coefficient in their thermoelastic damping formula $K=((1+\upsilon))/((1-2\upsilon))$, which is different from that of Lifshitz and Roukes (2000), in which υ is Poisson's

* Corresponding Author.
Email Address: naghamdi@uqu.edu.sa (N. A. Alghamdi)
https://doi.org/10.21833/ijaas.2023.12.015
Corresponding author's ORCID profile:
https://orcid.org/0000-0002-5796-3217

ratio. Many researchers have investigated nanobeam vibration and processes of heat transfer (Al-Huniti et al., 2001; Al-Lehaibi and Youssef, 2015; Boley, 1972; Kidawa-Kukla, 2003; Manolis and Beskos, 1980). Al-Lehaibi and Yossief (2015) studied the thermoelastic vibration of gold nanobeams subjected to thermal shock. Kidawa-Kukla (2003) used the properties of Green's function to study the internal and external damping effects on the lateral oscillations of the beam induced by the mobile heat source. Boley (1972) studied the effect of thermal shock on the vibration of a rectangular simply supported nanobeam. Manolis and Bescos (1980) used the numerical method to discuss the thermoelastic dynamic response of the nanobeam subjected to thermal loads. Al-Huniti et al. (2001) studied the displacements and stresses of a rod heated by a moving laser beam and the dynamic behavior using the Laplace transform method. Alghamdi (2020b) studied the thermoelastic vibration of micro/nanobeam subjected to a moving heat source. Youssef and Al Thobaiti (2022) studied the vibration of a thermoelastic nanobeam due to the thermo-electrical effect of graphene nano-strip under the Green-Naghdi type-II model. Alzahrani and Alghamdi (2023) studied the vibration of a nanobeam subjected to the constant magnetic field and ramp-type heat under non-Fourier heat conduction law based on the Lord-Shulman model.

This study uses Green-Naghdi theory type-I and III heat conduction law for the first time to analyze thermoelastic, homogeneous, isotropic nanobeams in the context of the non-Fourier law of heat conduction, where the first end of the nanobeam is based on a graphene strip connected to electricity current. A low voltage was applied to a graphene strip, and as a result of this current, Nanobeams were thermally loaded with heat from the graphene strip due to the thermal effect of electrical current. An electrical isolator with high thermal conductivity was used to electrically isolate the nanobeam, as shown in Fig. 1. This work is a novel application of an electrical field to a thermoelastic nanobeam under Green-Naghdi theory type-I and III, which has not been executed before, and therefore the results will be new.

2. Problem formulation

2.1. Model description

We consider the flexural deflections to be very small for thermoelastic thin nanobeam of thickness $h\left(-\frac{h}{2} \le z \le \frac{h}{2}\right)$, width $b\left(-\frac{b}{2} \le y \le \frac{b}{2}\right)$, and length $\ell(0 \le x \le \ell)$.

As in Fig. 1, the *x, y*, and *z*-axes are defined through the longitudinal ℓ, width b, and thickness h directions of the beam.

In an equilibrium state, the nanobeam has no damping, unstressed, unstrained, and the reference temperature is T_0 everywhere (Lee and Tsai, 2007).

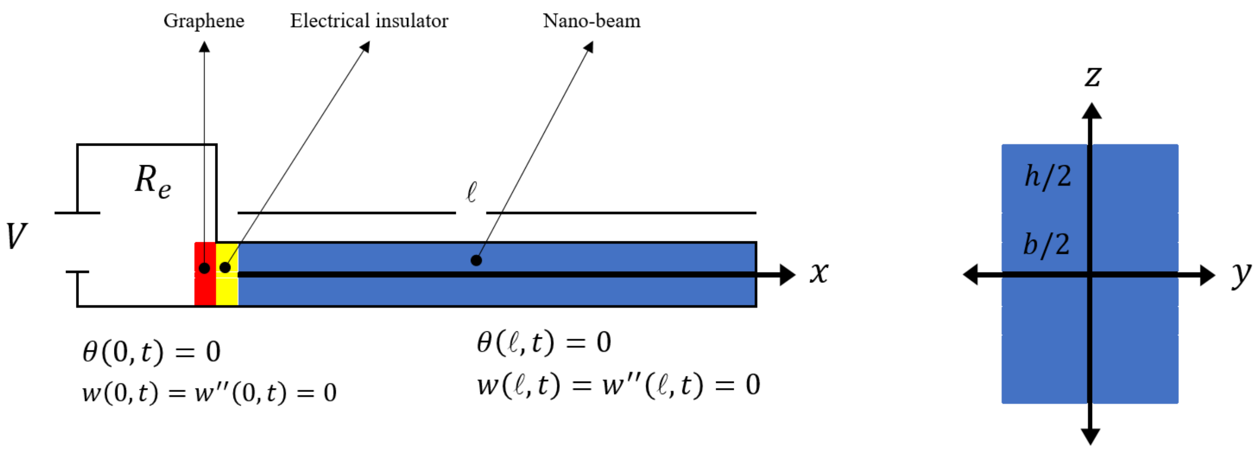

Fig. 1: Thermoelastic rectangular nanobeam

Euler-Bernoulli equation states that any plane cross-section perpendicular to the beam's axis (neutral surface) will remain so during beam bending (Grover, 2012).

Then, the displacement components will take the forms (Grover, 2012; 2013; 2015; Grover and Seth, 2018; 2019; Saanouni et al., 2004):

$$u(x,y,z,t) = -z\frac{\partial w(x,t)}{\partial x},\ v(x,y,z,t) = 0,\ w(x,y,z,t) = w(x,t) \tag{1}$$

The flexural moment of the cross-section and equation of motion are given (Grover, 2012; Grover and Seth, 2018; 2019; Saanouni et al., 2004):

$$M(x,t) = (\lambda + 2\mu)I\frac{\partial^2 w(x,t)}{\partial x^2} + \beta M_T(x,t) \tag{2}$$

where, the equation of motion is in the form:

$$\frac{\partial^2 M(x,t)}{\partial x^2} + \rho A\frac{\partial^2 w(x,t)}{\partial t^2} = 0 \tag{3}$$

The thermal moment M_T of the nanobeam about the x-axis is given (Grover, 2012; Grover and Seth, 2018; 2019; Saanouni et al., 2004):

$$M_T(x,t) = b\int_{-h/2}^{h/2} T(x,z,t) z dz \tag{4}$$

where, $I = \frac{bh^3}{12}$ gives the moment of inertia of the cross-section around the x-axis and $\beta = (3\lambda + 2\mu)\alpha_T$. Thus, the equation of motion, which gives thermally induced lateral vibrations of the nanobeam, takes the form (Grover and Seth, 2018):

$$(\lambda + 2\mu)I\frac{\partial^4 w(x,t)}{\partial x^4} + \rho A\frac{\partial^2 w(x,t)}{\partial t^2} + \beta\frac{\partial^2 M_T(x,t)}{\partial x^2} = 0 \tag{5}$$

where, $A = hb$ is the cross-section area. The heat conduction equations which have been proposed by Green-Naghdi take the following form (Green and Naghdi, 1993):

$$\left(\frac{\partial}{\partial t} + \frac{K_2}{K_1}\right)\nabla^2\theta(x,y,z,t) = \frac{\partial^2}{\partial t^2}\left(\frac{\rho C_v}{K_1}\theta(x,y,z,t) + \frac{\beta T_0}{K_1}e(x,y,z,t)\right) - \frac{1}{K_1}Q(x,y,z,t). \tag{6}$$

The unified Eq. 6 could be used for the two types of Green-Naghdi theories as follows:

(a) The setting $K_1 = K, K_2 = 0$ represents the Green-Naghdi type-I model.
(b) The setting $K_1 = K, K_2 = K^*$ represents the Green-Naghdi type-III model.

where, $K^* = \frac{(\lambda+2\mu)C_v}{4}$ is the characteristic of Green-Naghdi theory, K is the usual thermal conductivity, and Q is the heat source. The volumetric strain has the form:

$$e(x,z,t) = \frac{\partial u(x,z,t)}{\partial x} + \frac{\partial v(x,z,t)}{\partial y} + \frac{\partial w(x,z,t)}{\partial z} \tag{7}$$

thus, from Eqs. 1 and 7, we have:

$$\mathrm{e(x,z,t)} = -\mathrm{z}\frac{\partial^2 \mathrm{w(x,t)}}{\partial \mathrm{x}^2} \tag{8}$$

then, we obtain:

$$\sigma_{xx}(x,z,t) = (\lambda + 2\mu)e(x,z,t) - \beta\theta(x,z,t). \tag{9}$$

The upper and lower surfaces of the beam do not have heat transfer, so $\left.\frac{\partial T(x,z,t)}{\partial z}\right|_{z=\pm\frac{h}{2}} = 0$. Hence, for a nanobeam, we can assume the temperature depends on a $\sin(pz)$ function through the thickness direction of the beam, where $p = \frac{\pi}{h}$, which gives (Green and Naghdi, 1993):

$$\theta(x,z,t) = T(x,z,t) - T_0 = \varphi(x,t)\sin(pz) \tag{10}$$

and

$$\mathrm{Q(x,z,t) = q(x,t)\sin(pz)} \tag{11}$$

where, $\theta(x,z,t)$ is devoted to the temperature increment. Hence, from Eqs. 4, 5, and 10 we obtain:

$$\frac{\partial^4 w(x,t)}{\partial x^4} + \frac{12\rho}{h^2(\lambda+2\mu)}\frac{\partial^2 w(x,t)}{\partial t^2} + \frac{12\beta}{h^3(\lambda+2\mu)}\frac{\partial^2\varphi(x,t)}{\partial x^2}\int_{-h/2}^{h/2} z\sin(pz)dz = 0. \tag{12}$$

After doing the integrations, the Eq. 12 has the form:

$$\frac{\partial^4 w(x,t)}{\partial x^4} + \frac{12\rho}{h^2(\lambda+2\mu)}\ddot{w}(x,t) + \frac{24\beta}{h\pi^2(\lambda+2\mu)}\frac{\partial^2\varphi(x,t)}{\partial x^2} = 0. \tag{13}$$

Eq. 6 can be written as:

$$\left(\frac{\partial}{\partial t} + \frac{K_2}{K_1}\right)\left(\frac{\partial^2\theta}{\partial x^2} + \frac{\partial^2\theta}{\partial z^2}\right) = \frac{\rho C_r}{K_1}\frac{\partial^2\theta}{\partial t^2} + \frac{\beta T_0}{K_1}\frac{\partial^2 e}{\partial t^2} - \frac{1}{K_1}Q(x,z,t). \tag{14}$$

Substituting Eqs. 8, 10, and 11 into 14, we get

$$\left(\frac{\partial}{\partial t} + \frac{K_2}{K_1}\right)\left(\frac{\partial^2\varphi}{\partial x^2} - \varphi p^2\right)\sin(pz) = \frac{\partial^2}{\partial t^2}\left(\frac{\rho C_V}{K_1}\varphi\,\mathrm{sip}(pz) - \frac{\beta T_0}{K_1}z\frac{\partial^2 w}{\partial x^2}\right) - \frac{1}{K_1}q(x,t)\sin(pz). \tag{15}$$

In Eq. 15, both sides will be multiplied by z and will be integrated relating to z from

$\left(-\frac{h}{2}\right)$ *to* $\left(\frac{h}{2}\right)$,

then we obtain:

$$\left(\frac{\partial}{\partial t} + \frac{K_2}{K_1}\right)\left(\frac{\partial^2\varphi}{\partial x^2} - \varphi p^2\right) = \frac{\partial^2}{\partial t^2}\left(\varphi - \frac{\beta T_0}{\varepsilon K_1}\frac{\pi^2 h}{24}\frac{\partial^2 w}{\partial x^2}\right) - \frac{1}{K_1}q(x,t) \tag{16}$$

where, $\varepsilon = \frac{\rho C_v}{K_1}$. The Eq. 9 takes the form:

$$\sigma_{xx} = (\lambda + 2\mu)e - \beta\varphi\sin(pz) \tag{17}$$

2.2. Solution of the governing equations

The following non-dimensional variables will be used (Biot, 1955):

$$(x', w', h', \ell') = \varepsilon c_0(x, w, h, \ell), (t', \tau') = \varepsilon c_0^2(t, \tau), \sigma' = \frac{\sigma}{\lambda+2\mu}, \varphi' = \frac{\varphi}{T_0}, q' = \frac{q}{T_0 K\varepsilon^2 c_0^2}, c_0^2 = \frac{\lambda+2\mu}{\rho}. \tag{18}$$

Then, we have

$$\frac{\partial^4 w(x,t)}{\partial x^4} + \varepsilon_1\ddot{w}(x,t) + \varepsilon_2\frac{\partial^2\varphi(x,t)}{\partial x^2} = 0 \tag{19}$$

$$\left(\frac{\partial}{\partial t} + \frac{K_2}{K_1}\right)\left(\frac{\partial^2\varphi(x,t)}{\partial x^2} - \varepsilon_3\varphi(x,t)\right) = \frac{\partial^2}{\partial t^2}\left(\varphi(x,t) - \varepsilon_4\frac{\partial^2 w(x,t)}{\partial x^2}\right) - \frac{1}{K_1}q(x,t) \tag{20}$$

$$\sigma_{xx}(x,z,t) = e(x,z,t)\varepsilon_5 - \varphi(x,t)\sin(pz) \tag{21}$$

where,

$$\varepsilon_1 = \frac{12}{h^2}, \varepsilon_2 = \frac{24\beta T_0}{h\pi^2(\lambda+2\mu)}, \varepsilon_3 = p^2, \varepsilon_4 = \frac{\pi^2 h\beta}{24K\varepsilon},$$

and

$\varepsilon_5 = \frac{\beta T_0}{(\lambda+2\mu)}$.

2.3. Laplace transform solution

We will apply the Laplace transform with the following definition:

$$\bar{f}(x,s) = \int_0^\infty f(x,t)e^{-st}dt. \quad (22)$$

Then, the Eqs. 19-21 will take the following forms:

$$\frac{d^4\bar{w}}{dx^4} + \varepsilon_1 s^2 \bar{w} + \varepsilon_2 \frac{d^2\bar{\vartheta}}{dx^2} = 0 \quad (23)$$

$$\left(s + \frac{K_2}{K_1}\right)\left(\frac{d^2\bar{\varphi}}{dx^2} - \varepsilon_3\bar{\varphi}\right) = s^2\left(\bar{\varphi} - \varepsilon_4 \frac{d^2\bar{w}}{dx^2}\right) - \frac{1}{K_1}\bar{q} \quad (24)$$

$$\bar{\sigma}_{xx} = \bar{e} - \varepsilon_5 \bar{\varphi}\sin(pz) \quad (25)$$

and the Eq. 8 takes the form:

$$\bar{e} = -z\frac{d^2\bar{w}}{dx^2} \quad (26)$$

Assume that the beam is a conductor with electrical resistance $R_e(\Omega)$, and that it is being heated by a specific source due to the thermal effect of an electrical voltage connection (Joule's equation of electrical heating) $V(\mathrm{V})$. Then, Joule's equation of electrical heating is given by:

$$q(x,t) = \frac{V^2}{R_e}t. \quad (27)$$

Then, after applying the Laplace transform, we have:

$$\bar{q} = \frac{V^2}{R_e s^2} \quad (28)$$

which gives:

$$\left(s + \frac{K_2}{K_1}\right)\left(\frac{d^2\bar{\varphi}}{dx^2} - \varepsilon_3\bar{\varphi}\right) = s^2\left(\bar{\varphi} - \varepsilon_4 \frac{d^2\bar{w}}{dx^2}\right) - \frac{1}{K_1}\frac{V^2}{R_e s^2}. \quad (29)$$

We will re-write the Eqs. 23 and 24 in the form:

$$(D^4 + \varepsilon_1 s^2)\bar{w} + \varepsilon_2 D^2\bar{\varphi} = 0 \quad (30)$$

and

$$s^2\varepsilon_4 D^2\bar{w} + \left(D^2\left(s + \frac{K_2}{K_1}\right) - \left(s^2 + s\varepsilon_3 + \varepsilon_3\frac{K_2}{K_1}\right)\right)\bar{\varphi} = -\frac{1}{K_1}\frac{V^2}{R_e s^2} \quad (31)$$

or, we have

$$D^2\bar{w} + (\varepsilon_6 D^2 - \varepsilon_7)\bar{\varphi} = -\varepsilon_8 \quad (32)$$

where,

$D^r = \frac{d^r}{dx^r}$, $\tilde{K} = \frac{K_2}{K_1}$, $\varepsilon_6 = \frac{(s+\tilde{K})}{s^2\varepsilon_4}$, $\varepsilon_7 = \frac{(s^2+s\varepsilon_3+\varepsilon_3\tilde{K})}{s^2\varepsilon_4}$

and

$\varepsilon_8 = \frac{V^2}{K_1\varepsilon_4 R_e s^4}$.

Eliminating Eqs. 30 and 32, we obtain:

$$(D^6 - LD^4 + MD^2 - N)\bar{w} = 0 \quad (33)$$

and

$$(D^6 - LD^4 + MD^2 - N)\bar{\varphi} = -\psi \quad (34)$$

where,

$L = \frac{(\varepsilon_7+\varepsilon_2)}{\varepsilon_6}$, $M = \varepsilon_1 s^2$, $N = \frac{\varepsilon_1\varepsilon_7 s^2}{\varepsilon_6}$, and $\psi = \frac{\varepsilon_1\varepsilon_8 s^2}{\varepsilon_6}$.

The general solution of the Eq. 33 is as follows:

$$\bar{w} = \sum_{j=1}^{3} A_j \sinh\left(k_j(\ell - x)\right). \quad (35)$$

The general solution of the Eq. 34 is as follows:

$$\bar{\varphi} = \frac{\psi}{N} + \sum_{j=1}^{3} B_j \sinh\left(k_j(\ell - x)\right) \quad (36)$$

where, $\pm k_1, \pm k_2, \pm k_3$ are the roots of the characteristic equation

$$k^6 - Lk^4 + Mk^2 - N = 0. \quad (37)$$

To get the relation between the parameters A_j and B_j, we use the relation in (30), which gives:

$$(K_j^4 + \varepsilon_1 s^2)A_j + \varepsilon_2 K_j^2 B_j = 0,\ j = 1,2,3. \quad (38)$$

Then we have:

$$\bar{\varphi} = \frac{\psi}{N} - \frac{1}{\varepsilon_2}\sum_{j=1}^{3}\frac{(K_j^4+\varepsilon_1 s^2)}{K_j^2}A_j \sinh\left(k_j(\ell - x)\right). \quad (39)$$

Applying the boundary conditions in Eqs. 35 and 36, we get (Youssef and Al Thobaiti, 2022):

$$\sum_{j=1}^{3} A_j \sinh(k_j\ell) = 0 \quad (40)$$

$$\sum_{j=1}^{3} k_j^2 A_j \sinh(k_j\ell) = 0 \quad (41)$$

and

$$\sum_{j=1}^{3}\frac{(K_j^4+\varepsilon_1 s^2)}{K_j^2}A_j \sinh(k_j\ell) = \frac{\varepsilon_2\psi}{N}. \quad (42)$$

Then, by solving the Eqs. 40-42, we get the parameters A_1, A_2, A_3 as follows:

$$A_1 = \frac{k_1^2k_2^2k_3^2\varepsilon_2\psi}{\varepsilon_1 s^2(k_1^2-k_2^2)(k_1^2-k_3^2)N\sinh(k_1\ell)},$$

$$A_2 = \frac{k_1^2k_2^2k_3^2\varepsilon_2\psi}{\varepsilon_1 s^2(k_2^2-k_1^2)(k_2^2-k_3^2)N\sinh(k_2\ell)}$$

and

$$A_3 = \frac{k_1^2k_2^2k_3^2\varepsilon_2\psi}{\varepsilon_1 s^2(k_3^2-k_1^2)(k_3^2-k_2^2)N\sinh(k_3\ell)}.$$

That completes the solution of the Laplace transform domain. The lateral deflection function is as follows:

$$\bar{w}(x,s)=\frac{\varepsilon_2\psi}{\varepsilon_1 s^2}\begin{bmatrix}\frac{k_1^2k_2^2k_3^2\sinh(k_1(\ell-x))}{(k_1^2-k_2^2)(k_1^2-k_3^2)N\sinh(k_1\ell)}+\\ \frac{k_1^2k_2^2k_3^2\sinh(k_2(\ell-x))}{(k_2^2-k_1^2)(k_2^2-k_3^2)N\sinh(k_2\ell)}+\\ \frac{k_1^2k_2^2k_3^2\sinh(k_3(\ell-x))}{(k_3^2-k_1^2)(k_3^2-k_2^2)N\sinh(k_3\ell)}\end{bmatrix} \tag{43}$$

and the temperature increment function is as follows:

$$\bar{\theta}(x,s)=\frac{\psi\sin(pz)}{\frac{\varepsilon_1\varepsilon_7 s^2}{\varepsilon_6}}+\frac{\psi\sin(pz)}{\varepsilon_1 s^2}\begin{bmatrix}\frac{(K_1^4+\varepsilon_1 s^2)k_1^2k_2^2k_3^2\sinh(k_1(\ell-x))}{K_1^2(k_1^2-k_2^2)(k_1^2-k_3^2)\,\mathrm{N}\sinh(k_1\ell)}+\\ \frac{(K_2^4+\varepsilon_1 s^2)k_1^2k_2^2k_3^2\sinh(k_2(\ell-x))}{K_2^2(k_2^2-k_1^2)(k_2^2-k_3^2)\,\mathrm{N}\sinh(k_2\ell)}+\\ \frac{(K_3^4+\varepsilon_1 s^2)k_1^2k_2^2k_3^2\sinh(k_3(\ell-x))}{K_3^2(k_3^2-k_1^2)(k_3^2-k_2^2)\,\mathrm{N}\sinh(k_3\ell)}\end{bmatrix}. \tag{44}$$

The strain takes the form:

$$\bar{e}(x,z,s)=\frac{-z\varepsilon_2\psi}{\varepsilon_1 s^2}\begin{bmatrix}\frac{k_1^2k_2^2k_3^2k_1^2\sinh(k_1(\ell-x))}{(k_1^2-k_2^2)(k_1^2-k_3^2)\,\mathrm{N}\sinh(k_1\ell)}+\\ \frac{k_1^2k_2^2k_3^2k_2^2\sinh(k_2(\ell-x))}{(k_2^2-k_1^2)(k_2^2-k_3^2)\,\mathrm{N}\sinh(k_2\ell)}+\\ \frac{k_1^2k_2^2k_3^2k_3^2\sinh(k_3(\ell-x))}{(k_3^2-k_1^2)(k_3^2-k_2^2)\,\mathrm{N}\sinh(k_3\ell)}\end{bmatrix}. \tag{45}$$

The strain-energy density function through the nanobeam is given by Elsibai* and Youssef (2011):

$$\varpi(x,z,t)=\sum_{i,j}^{3}\frac{1}{2}\sigma_{ij}(x,z,t)e_{ij}(x,z,t)=\frac{1}{2}\sigma(x,z,t)e(x,z,t) \tag{46}$$

2.4. Numerical inversion of the Laplace transform

In order to obtain the expressions of the studied domain variables in the time domain, it is necessary to apply the inverse of the Laplace Transform. Obtaining these conversions may take a long time and be tedious. Numerical algorithms and approximate methods are used in this case. By using the following Riemann sum approximation formula, any function $f(x,s)$ in the Laplace domain will be inverted into a function $f(x,t)$ (Honig and Hirdes, 1984).

$$\mathrm{L}^{-1}\left(\bar{\mathrm{f}}(\mathrm{s})\right)=\mathrm{f}(\mathrm{t})\approx\frac{\mathrm{e}^{\upsilon t}}{\mathrm{t}}\left[\frac{1}{2}\bar{\mathrm{f}}(\upsilon)+\mathrm{Re}\sum_{\mathrm{n}=1}^{\mathrm{N}}(-1)^{\mathrm{n}}\bar{\mathrm{f}}\left(\upsilon+\frac{\mathrm{i}\mathrm{n}\pi}{\mathrm{t}}\right)\right], \tag{47}$$

where, Re represents the real part, while i represents the imaginary part. For faster convergence, several experiments confirmed that υ can satisfy the relation $\upsilon t\approx 4.7$.

3. Numerical results

Since copper is used as a thermoelastic material, the following values with various physical constants have been used (Youssef and Al Thobaiti, 2022):

$\alpha_T=1.78(10)^{-5}\ \mathrm{K}^{-1}, \rho=8954\ \mathrm{kg\ m}^{-3}$, $T_0=300\ \mathrm{K}, C_v=383.1\mathrm{Jkg}^{-1}\ \mathrm{K}^{-1}$, $\lambda=77.6\times10^{9}\ \mathrm{N\ m}^{-2}$, $\mu=38.6\times10^{9}\mathrm{Nm}^{-2}, K=386\mathrm{Wm}^{-1}K^{-1}$.

The electrical resistance of graphene in the nanoscale has values $R_e=500\Omega$ (Nirmalraj et al., 2011). The aspect ratios of the nanobeam are fixed as $\ell/h=8$ and $b=h/2$. We will take the range of the nanobeam length $\ell(1-100)\times10^{-12}$ m, and the original time t of order 10^{-12}sec. The figures were organized by using the dimensionless variables for nanobeam length $\ell=1.0$, $\theta_0=1.0$, $z=h/4$, and $t=1.0$. The situation $\tilde{K}=0$ represents the Green-Naghdi type-I model, while the situation

$$\tilde{K}=\frac{K^*}{K}=\frac{(\lambda+2\mu)C_v}{4K}$$

represents the Green-Naghdi type-III model.

4. Discussion

Two groups of figures show the numerical results of the problem; the first group represents the distributions of the temperature increment, vibration (lateral deflection), cubical deformation, stress, and strain-energy density when the graphene nanostrip's electrical resistance value is constant and equal to the value Res $=500\Omega$ and for three different electrical voltage values $V=(1.0,1.1,1.2)$V. While the second group represents the distributions of the same functions when the graphene nanostrip's electrical voltage value is constant and equal to the value $V=1.0$ V and for three different electrical resistance values Res $=(500,550,600)\Omega$.

Figs. 2a and 2b represent the temperature increment with respect to x due to the various values of an electrical voltage in the case of the Green-Naghdi type-I and type-III model, respectively. It is observed that an increase in an electrical voltage results in an increase in the temperature increment.

Figs. 3a and 3b represent the vibration (lateral deflection) with respect to x due to the various values of an electrical voltage in the case of the Green-Naghdi type-I and type-III models, respectively. It is observed that an increase in an electrical voltage results in an increase in the lateral deflection (vibration).

Figs. 4a and 4b represent cubical deformation (strain) with respect to x due to the various values of an electrical voltage in the case of the Green-Naghdi type-I and type-III model, respectively. It is observed that an increase in electrical voltage results in an increase in the strain's absolute value (the cubical deformation).

Figs. 5a and 5b represent stress with respect to x due to the various values of an electrical voltage in the case of the Green-Naghdi type-I and type-III model, respectively. It is observed that an increase in an electrical voltage results in an increase in the stress's absolute value.

Figs. 6a and 6b represent strain energy density with respect to x due to the various values of an electrical voltage in the case of the Green-Naghdi type-I and type-III model, respectively. It is observed that an increase in an electrical voltage results in an increase in the strain energy density's absolute value. This means that both the vibration and the temperature increment that has been produced along the nanobeam can be tuned using electrical voltage.

Figs. 7a and 7b represent the temperature increment with respect to x due to the various values of electrical resistance in the case of the Green-Naghdi type-I and type-III model, respectively. It is observed that an increase in electrical resistance results in a decrease in the temperature increment.

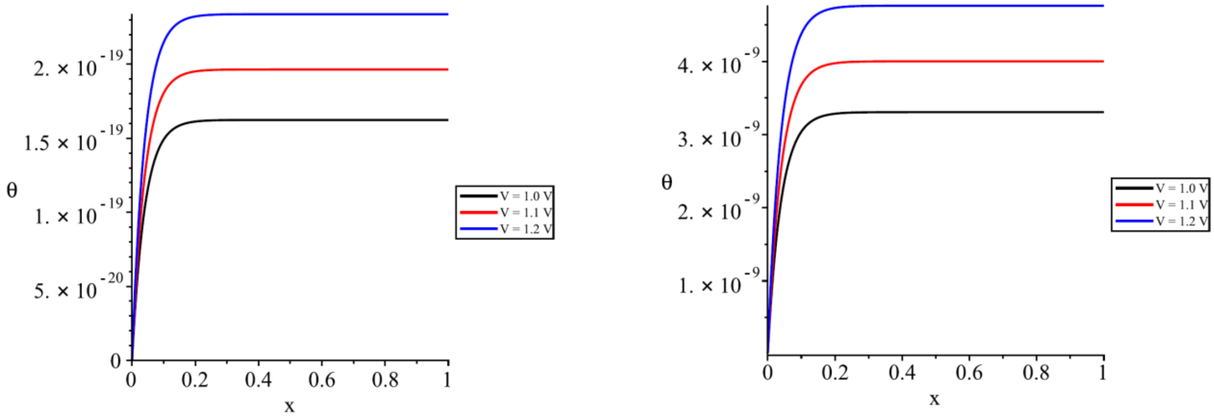

a: type-I model when Res = 500Ω   b: type-III model when Res=500Ω

Fig. 2: The temperature increment in the case of the Green-Naghdi

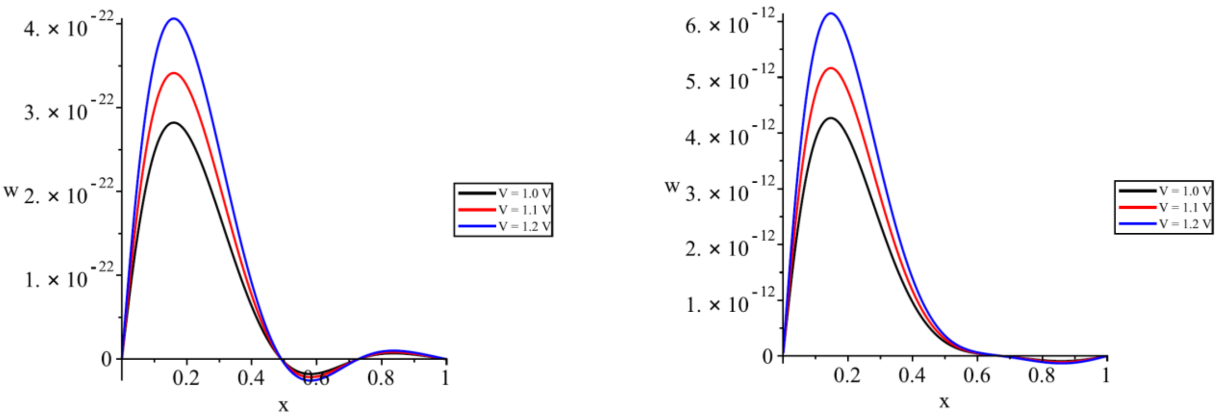

a: type-I model when Res = 500Ω   b: type-III model when Res = 500Ω

Fig. 3: The lateral deflection in the case of the Green-Naghdi

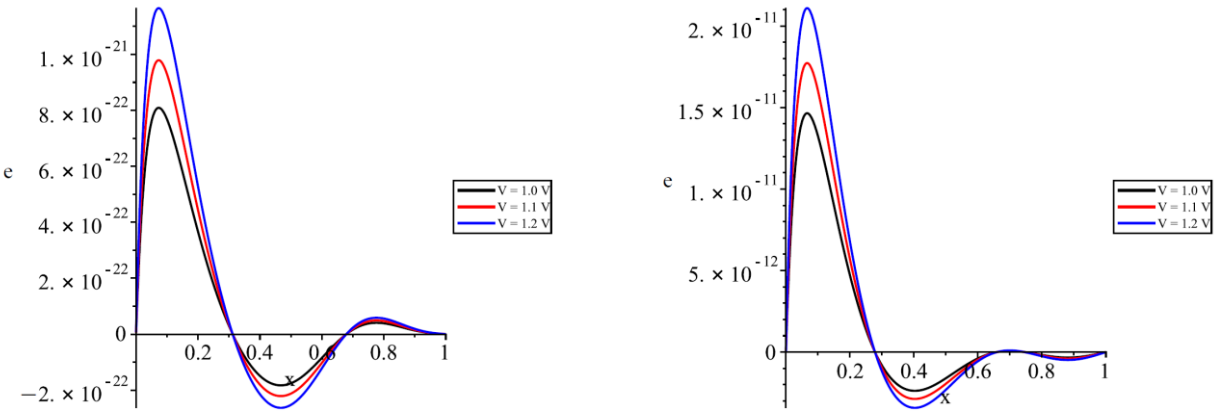

a: type-I model when Res = 500Ω   b: type-III model when Res = 500Ω

Fig. 4: The volumetric deformation in the case of the Green-Naghdi

Figs. 8a and 8b represent the vibration (lateral deflection) with respect to x due to the various values of electrical resistance in the case of the Green-Naghdi type-I and type-III model, respectively. It is observed that an increase in an electrical resistance result in decrease in the lateral deflection (vibration). Figs. 9a and 9b represent cubical deformation (strain) with respect to x due to the various values of electrical resistance in the case of the Green-Naghdi type-I and type-III models, respectively. It is observed that an increase in electrical resistance results in a decrease in the strain's absolute value (the cubical deformation).

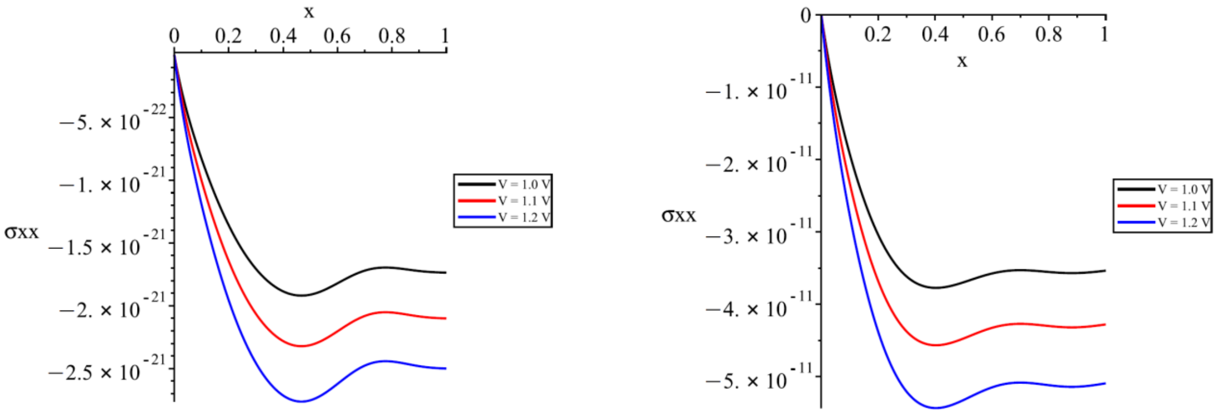

a: type-I model when Res = 500Ω b: type-III model when Res = 500Ω

Fig. 5: The stress component in the case of the Green-Naghdi

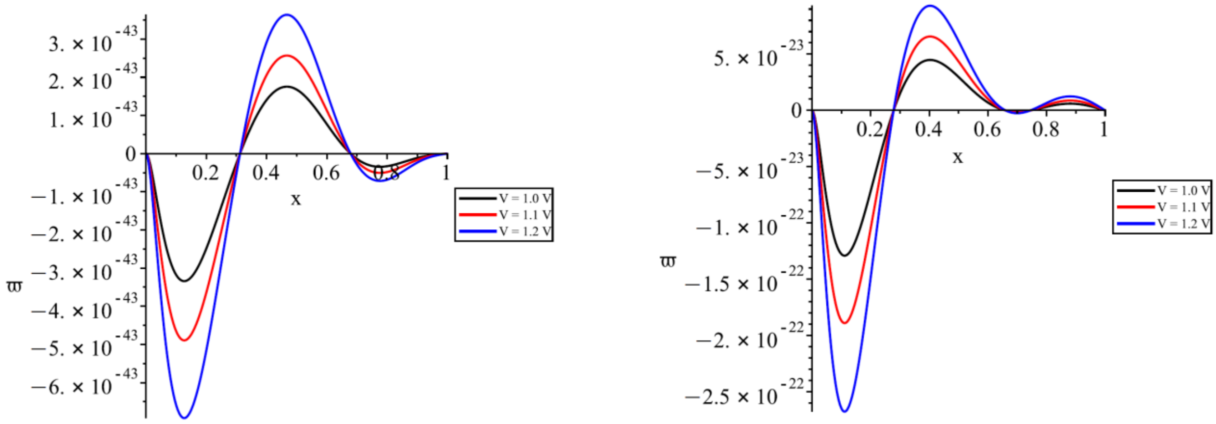

a: type-I model when Res = 500Ω b: type-III model when Res = 500Ω

Fig. 6: The strain energy density in the case of the Green-Naghdi

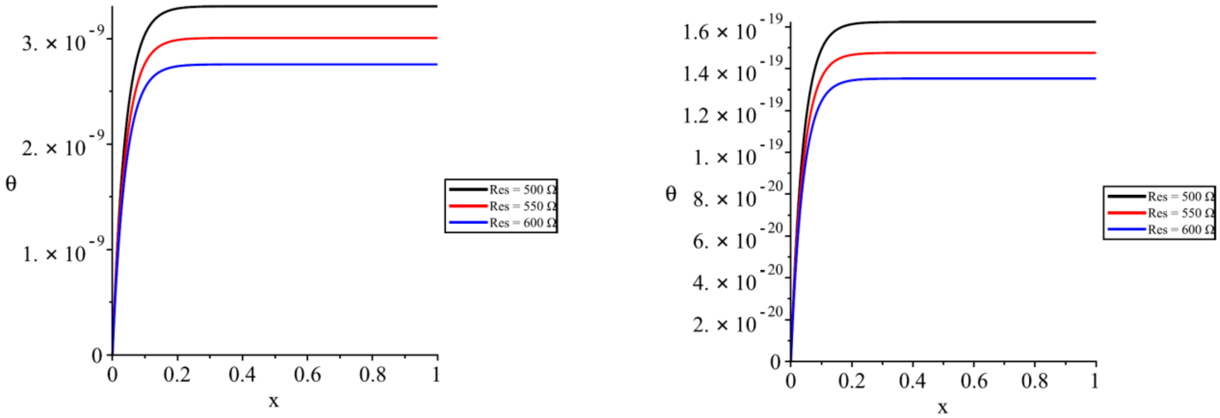

a: type-I model when $V = 1.0$ V b: type-III model when $V = 1.0$ V

Fig. 7: The temperature increment in the case of the Green-Naghdi

Figs. 10a and 10b represent stress with respect to x due to the various values of electrical resistance in the case of the Green-Naghdi type-I and type-III models, respectively. It is observed that an increase in electrical resistance results in a decrease in the stress's absolute value.

Figs. 11a and 11b represent strain energy density with respect to x due to the various values of electrical resistance in the case of the Green-Naghdi type-I and type-III models, respectively. It is observed that an increase in electrical resistance results in a decrease in the strain energy density's absolute value. Thismeans that both the vibration and the temperature increment that has been produced along the nanobeam can be tuned using electrical resistance.

5. Conclusion

In this work, we studied thermoelastic nanobeams using non-Fourier conducted heat. At the first end of the nanobeam, nanostrip graphene is linked by a low voltage electrical current. The generalization theory of thermoelasticity's Lord-Shulman model was used. The nanobeam was thermally stressed by a low voltage current flowing over the graphene nanostrip. It was found that all the functions investigated are significantly influenced by voltage and resistance. The nano-strip of graphene could be used as a tuner to control the vibration and thermal increment of the nanobeam by controlling its electrical voltage and electrical resistance.

Overall, the results showed that the Green-Naghdi type-I and III model agrees with the physical behavior of graphene strips and copper nanobeam. These results are in agreement with references such as (Abouelregal, 2022; Al-Lehaibi and Youssef, 2015; Alzahrani and Alghamdi, 2023; Grover, 2012; Grover and Seth, 2019; Manolis and Beskos, 1980; Sharma and Grover, 2011; Youssef and Salem, 2022; Zakaria et al., 2022). We will apply an electrical voltage as a heat source on a variety of beam types and in various heat conduction laws in future work.

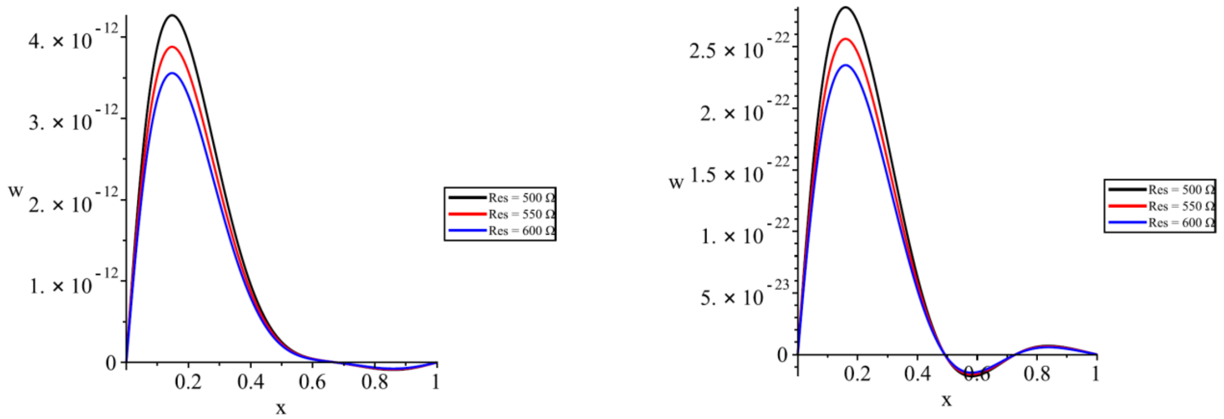

a: type-I model when $V = 1.0$ V   b: type-III model when $V = 1.0$ V

Fig. 8: The lateral deflection in the case of the Green-Naghdi

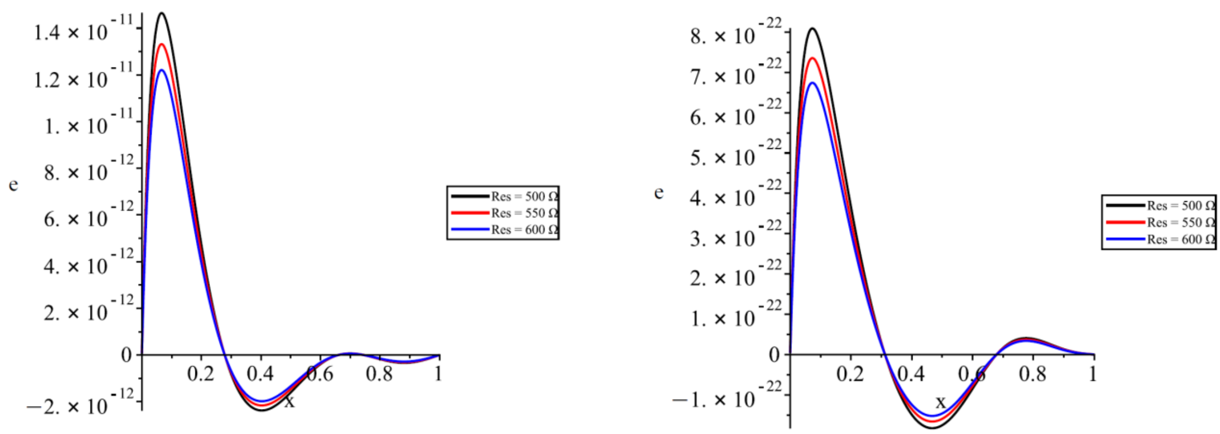

a: type-I model when $V = 1.0$ V   b: type-III model when $V = 1.0$ V

Fig. 9: The volumetric deformation in the case of the Green-Naghdi

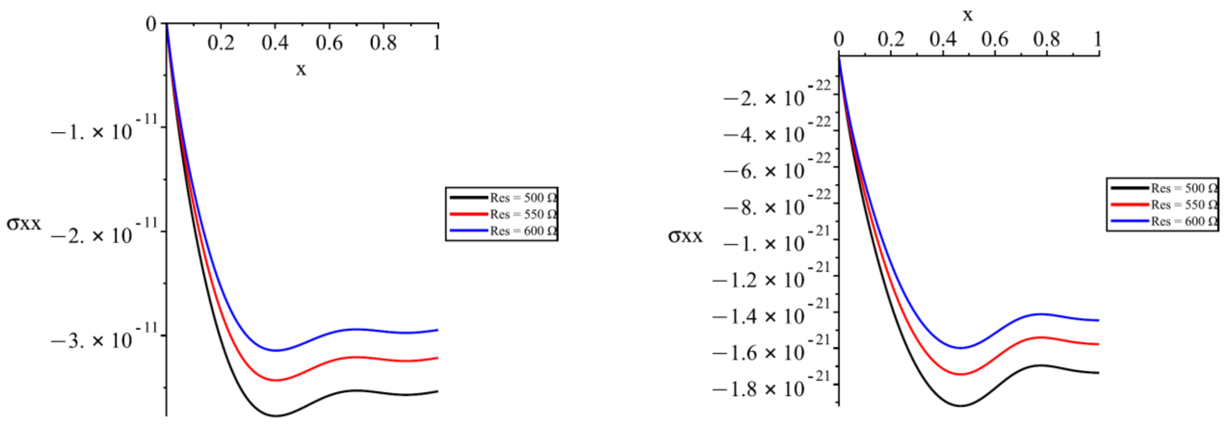

a: type-I model when $V = 1.0$ V   b: type-III model when $V = 1.0$ V

Fig. 10: The stress component in the case of the Green-Naghdi

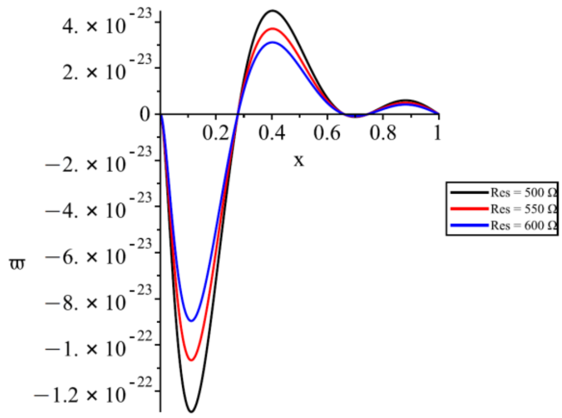

a: type-I model when $V = 1.0$ V

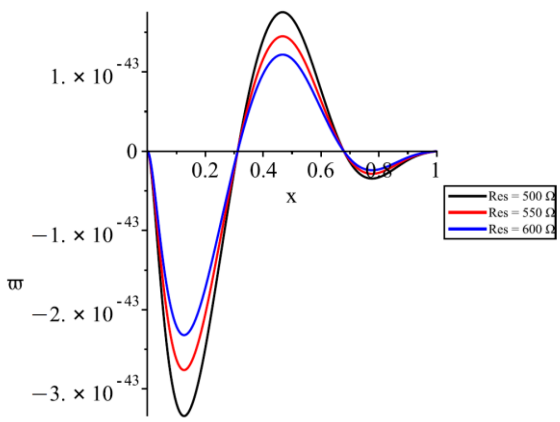

b: type-III model when $V = 1.0$ V

Fig. 11: The strain energy density in the case of the Green-Naghdi

List of symbols

M_T	Thermal moment
I	Moment of inertia
u, v, w	Displacement components
M	Flexural moment
K	Thermal conductivity
Q	Heat source
θ	Temperature increment
K^*	Characteristic of Green-Naghdi theory
$R_e(\Omega)$	Electrical resistance
V(V)	Electrical voltage
e	Strain
σ_{xx}	Stress
ω	Strain-energy density
α_T	Coefficient of linear thermal expansion
ρ	Density
T_0	Reference temperature
λ, μ	Lamè's parameter

Compliance with ethical standards

Conflict of interest

The author(s) declared no potential conflicts of interest with respect to the research, authorship, and/or publication of this article.

References

Abouelregal AE (2022). An advanced model of thermoelasticity with higher-order memory-dependent derivatives and dual time-delay factors. Waves in Random and Complex Media, 32(6): 2918-2939. https://doi.org/10.1080/17455030.2020.1871110

Alghamdi NA (2016). Two-temperature thermoelastic damping in rectangular microplate resonators. Journal of Computational and Theoretical Nanoscience, 13(11): 8375-8382. https://doi.org/10.1166/jctn.2016.5984

Alghamdi NA (2020a). The vibration of a viscothermoelastic nanobeam of silicon nitride based on dual-phase-lage heat conduction model and subjected to ramp-type heating. AIP Advances, 10(10): 105112. https://doi.org/10.1063/5.0026255

Alghamdi NA (2020b). The vibration of nano-beam subjected to thermal shock and moving heat source with constant speed. Journal of Nano Research, 61: 136-150. https://doi.org/10.4028/www.scientific.net/JNanoR.61.136

Alghamdi NA and Youssef HM (2017). Dual-phase-lagging thermoelastic damping in-extensional vibration of rotating nano-ring. Microsystem Technologies, 23: 4333-4343. https://doi.org/10.1007/s00542-017-3294-z

Al-Huniti NS, Al-Nimr MA, and Naji M (2001). Dynamic response of a rod due to a moving heat source under the hyperbolic heat conduction model. Journal of Sound and Vibration, 242(4): 629-640. https://doi.org/10.1006/jsvi.2000.3383

Al-Lehaibi EA and Youssef HM (2015). Vibration of gold nano-beam with variable young's modulus due to thermal shock. World Journal of Nano Science and Engineering, 5(04): 194. https://doi.org/10.4236/wjnse.2015.54020

Alzahrani MSJ and Alghamdi NA (2023). The vibration of a nanobeam subjected to constant magnetic field and ramp-type heat under non-Fourier heat conduction law based on the Lord-Shulman model. Advances in Mechanical Engineering, 15(5). https://doi.org/10.1177/16878132231177985

Biot M (1955). Variational principles in irreversible thermodynamics with application to viscoelasticity. Physical Review, 97(6): 1463. https://doi.org/10.1103/PhysRev.97.1463

Biot MA (1956). Thermoelasticity and irreversible thermodynamics. Journal of Applied Physics, 27(3): 240-253. https://doi.org/10.1063/1.1722351

Boley BA (1972). Approximate analyses of thermally induced vibrations of beams and plates. Journal of Applied Mechanics, 39(1): 212-216. https://doi.org/10.1115/1.3422615

Dhaliwal RS and Sherief HH (1980). Generalized thermoelasticity for anisotropic media. Quarterly of Applied Mathematics, 38(1): 1-8. https://doi.org/10.1090/qam/575828

Elsibai KA and Youssef HM (2011). State-space approach to vibration of gold nano-beam induced by ramp type heating without energy dissipation in femtoseconds scale. Journal of Thermal Stresses, 34(3): 244-263. https://doi.org/10.1080/01495739.2010.545737

Green AE and Naghdi P (1993). Thermoelasticity without energy dissipation. Journal of Elasticity, 31(3): 189-208. https://doi.org/10.1007/BF00044969

Grover D (2012). Viscothermoelastic vibrations in micro-scale beam resonators with linearly varying thickness. Canadian Journal of Physics, 90(5): 487-496. https://doi.org/10.1139/p2012-044

Grover D (2013). Transverse vibrations in micro-scale viscothermoelastic beam resonators. Archive of Applied Mechanics, 83: 303-314. https://doi.org/10.1007/s00419-012-0656-y

Grover D (2015). Damping in thin circular viscothermoelastic plate resonators. Canadian Journal of Physics, 93(12): 1597-1605. https://doi.org/10.1139/cjp-2014-0575

Grover D and Seth RK (2018). Viscothermoelastic micro-scale beam resonators based on dual-phase lagging model. Microsystem Technologies, 24: 1667-1672. https://doi.org/10.1007/s00542-017-3515-5

Grover D and Seth RK (2019). Generalized viscothermoelasticity theory of dual-phase lagging model for damping analysis in circular micro-plate resonators. Mechanics of Time-Dependent Materials, 23: 119-132. https://doi.org/10.1007/s11043-018-9388-x

Hoang CM (2015). Thermoelastic damping depending on vibration modes of nano beam resonator. Communications Physics, 25(4): 317-325. https://doi.org/10.15625/0868-3166/25/4/6887

Honig G and Hirdes U (1984). A method for the numerical inversion of Laplace transforms. Journal of Computational and Applied Mathematics, 10(1): 113-132. https://doi.org/10.1016/0377-0427(84)90075-X

Kidawa-Kukla J (2003). Application of the Green functions to the problem of the thermally induced vibration of a beam. Journal of Sound and Vibration, 262(4): 865-876. https://doi.org/10.1016/S0022-460X(02)01133-1

Lee YM and Tsai TW (2007). Ultra-fast pulse-laser heating on a two-layered semi-infinite material with interfacial contact conductance. International Communications in Heat and Mass Transfer, 34(1): 45-51. https://doi.org/10.1016/j.icheatmasstransfer.2006.08.017

Lifshitz R and Roukes ML (2000). Thermoelastic damping in micro-and nanomechanical systems. Physical Review B, 61(8): 5600. https://doi.org/10.1103/PhysRevB.61.5600

Lord HW and Shulman Y (1967). A generalized dynamical theory of thermoelasticity. Journal of the Mechanics and Physics of Solids, 15(5): 299-309. https://doi.org/10.1016/0022-5096(67)90024-5

Manolis GD and Beskos D (1980). Thermally induced vibrations of beam structures. Computer Methods in Applied Mechanics and Engineering, 21(3): 337-355. https://doi.org/10.1016/0045-7825(80)90101-2

Naik AK, Hanay MS, Hiebert WK, Feng XL, and Roukes ML (2009). Towards single-molecule nanomechanical mass spectrometry. Nature Nanotechnology, 4(7): 445-450. https://doi.org/10.1038/nnano.2009.152 **PMid:19581898 PMCid:PMC3846395**

Nirmalraj PN, Lutz T, Kumar S, Duesberg GS, and Boland JJ (2011). Nanoscale mapping of electrical resistivity and connectivity in graphene strips and networks. Nano Letters, 11(1): 16-22. https://doi.org/10.1021/nl101469d **PMid:21128677**

O'Connell AD, Hofheinz M, Ansmann M, Bialczak RC, Lenander M, Lucero E, and Cleland AN (2010). Quantum ground state and single-phonon control of a mechanical resonator. Nature, 464(7289): 697-703. https://doi.org/10.1038/nature08967 **PMid:20237473**

Saanouni K, Mariage JF, Cherouat A, and Lestriez P (2004). Numerical prediction of discontinuous central bursting in axisymmetric forward extrusion by continuum damage mechanics. Computers and Structures, 82(27): 2309-2332. https://doi.org/10.1016/j.compstruc.2004.05.018

Sharma JN, and Grover D (2011). Thermoelastic vibrations in micro-/nano-scale beam resonators with voids. Journal of Sound and Vibration, 330(12): 2964-2977. https://doi.org/10.1016/j.jsv.2011.01.012

Sun Y and Saka M (2010). Thermoelastic damping in micro-scale circular plate resonators. Journal of Sound and Vibration, 329(3): 328-337. https://doi.org/10.1016/j.jsv.2009.09.014

Tzou DY (1989). On the thermal shock wave induced by a moving heat source. Journal of Heat Transfer, 111(2): 232-238. https://doi.org/10.1115/1.3250667

Van Beek JTM and Puers R (2011). A review of MEMS oscillators for frequency reference and timing applications. Journal of Micromechanics and Microengineering, 22(1): 013001. https://doi.org/10.1088/0960-1317/22/1/013001

Youssef HM and Al Thobaiti AA (2022). The vibration of a thermoelastic nanobeam due to thermo-electrical effect of graphene nano-strip under Green-Naghdi type-II model. Journal of Engineering and Thermal Sciences, 2(1): 1-12. https://doi.org/10.21595/jets.2022.22568

Youssef HM and Alghamdi NA (2015). Thermoelastic damping in nanomechanical resonators based on two-temperature generalized thermoelasticity theory. Journal of Thermal Stresses, 38(12): 1345-1359. https://doi.org/10.1080/01495739.2015.1073541

Youssef HM and Salem RA (2022). The dual-phase-lag bioheat transfer of a skin tissue subjected to thermo-electrical shock. Journal of Engineering and Thermal Sciences, 2(2): 114-123. https://doi.org/10.21595/jets.2022.22945

Zakaria K, Sirwah MA, Abouelregal AE, and Rashid AF (2022). Photothermoelastic survey with memory-dependent response for a rotating solid cylinder under varying heat flux via dual phase lag model. Pramana, 96(4): 219. https://doi.org/10.1007/s12043-022-02452-6